Self-Assembly of Virus-Structured High Surface Area Nanomaterials and Their Application as Battery Electrodes

Elizabeth Royston,[†,‡] Ayan Ghosh,[§] Peter Kofinas,[||] Michael T. Harris,[†] and James N. Culver*[,‡]

School of Chemical Engineering, Purdue University, West Lafayette, Indiana 47907, Center for Biosystems Research, University of Maryland Biotechnology Institute, and Department of Chemical and Biomolecular Engineering and Fischell Department of Bioengineering, University of Maryland, College Park, Maryland 20742

Received June 4, 2007. In Final Form: October 12, 2007

High area nickel and cobalt surfaces were assembled using modified *Tobacco mosaic virus* (TMV) templates. Rod-shaped TMV templates (300 × 18 nm) engineered to encode unique cysteine residues were self-assembled onto gold patterned surfaces in a vertically oriented fashion, producing a >10-fold increase in surface area. Electroless deposition of ionic metals onto surface-assembled virus templates produced uniform metal coatings up to 40 nm in thickness. Within a nickel−zinc battery system, the incorporation of virus-assembled electrode surfaces more than doubled the total electrode capacity. When combined, these findings demonstrate that surface-assembled virus templates provide a robust platform for the fabrication of oriented high surface area materials.

Introduction

High surface area nanostructured materials have uses in an array of applications including electrodes, catalyst supports, thermal barriers, sensor arrays, and energy storage devices. Increased surface areas are generally achieved through the synthesis of particles with high surface to volume ratios or the manufacture of nanostructured materials from bulk substrates.[1,2] Methods used to create high surface area nanostructures, such as laser ionization or lithography, generally require complex and expensive technologies that can limit the application of these materials. To avoid such limitations, researchers are increasingly investigating alternative methods for the self-assembly of high surface area nanostructured materials and devices. One approach is templating materials onto biologically derived substrates. Biological templates such as nucleic acids and viruses have evolved to self-assemble into hierarchically ordered structures with high surface to volume aspects, making them ideal for the synthesis of high surface area nanomaterials. Previous studies have functionalized DNA,[3] virus particles[4] and protein tubules[5−8] using a variety of methods to produce field effect transistors,[9] battery electrodes,[10] and memory devices.[11] In contrast, the assembly and attachment of biologicals onto device surfaces has been difficult to accomplish. Recent work has shown that electrostatically induced alignments of uniform macromolecules such as viruses can be used to produce two-dimensional monolayers of biological templates.[12] However, the assembly and surface attachment of biologicals has primarily relied on the random association of biotemplates onto device surfaces. The arbitrary nature of this process can limit the usefulness of biotemplates in device assembly and represents a significant obstacle in creating high surface area nanostructured materials. Thus, there is a need to develop new methodologies for the oriented and uniform assembly of biotemplates onto device surfaces.

The use of biological components in nanostructured materials also requires the development of strategies to functionalize these components upon assembly. One area of particular interest is the development of methods to obtain continuous and uniform coatings of reactive metals. Most deposition strategies rely on the reduction of metal directly onto the surface of the biological template.[13−18] This methodology typically produces discrete metal particles that decorate the surface of the biotemplate, but often lack the uniformity needed to produce highly conductive surfaces. Chemical modifications to the surface of the biological tem-

* Corresponding author: James N. Culver, Center for Biosystems Research, University of Maryland Biotechnology Institute, College Park, MD 20742. Phone: (301) 405-2912. Fax: (301) 314-9075. E-mail: jculver@umd.edu.

[†] Purdue University.

[‡] Center for Biosystems Research, University of Maryland Biotechnology Institute.

[§] Department of Chemical and Biomolecular Engineering, University of Maryland.

[||] Fischell Department of Bioengineering, University of Maryland.

(1) Wang, P. *Curr. Opin. Biotechnol.* **2006**, *17*, 574−579.

(2) Yang, S. M.; Jang, S. G.; Choi, D. G.; Kim, S.; Yu, H. K. *Small* **2006**, *2* (4), 458−475.

(3) Braun, E.; Eichen, Y.; Sivan, U.; Ben-Yoseph, G. *Nature (London)* **1998**, *391* (6669), 775−778.

(4) Flynn, C. E.; Lee, S. W.; Peelle, B. R.; Belcher, A. M. *Acta Mater.* **2003**, *51* (19), 5867−5880.

(5) Mertig, M.; Kirsch, R.; Pompe, W. *Appl. Phys. A* **1998**, *66*, S723−S727.

(6) Behrens, S.; Wu, J.; Habicht, W.; Unger, E. *Chem. Mater.* **2004**, *16* (16), 3085−3090.

(7) Gao, X. Y.; Matsui, H. *Adv. Mater.* **2005**, *17* (17), 2037−2050.

(8) Matsui, H.; Pan, S.; Gologan, B.; Jonas, S. H. *J. Phys. Chem. B* **2000**, *104* (41), 9576−9579.

(9) Keren, K.; Berman, R. S.; Buchstab, E.; Sivan, U.; Braun, E. *Science* **2003**, *302* (5649), 1380−1382.

(10) Nam, K. T.; Kim, D. W.; Yoo, P. J.; Chiang, C. Y.; Meethong, N.; Hammond, P. T.; Chiang, Y. M.; Belcher, A. M. *Science* **2006**, *312* (5775), 885−888.

(11) Tseng, R. J.; Tsai, C. L.; Ma, L. P.; Ouyang, J. Y. *Nat. Nanotechnol.* **2006**, *1* (1), 72−77.

(12) Yoo, P. J.; Nam, K. T.; Qi, J.; Lee, S.-K.; Park, J.; Belcher, A. M.; Hammond, P. T. *Nat. Mater.* **2006**, *5* (3), 234−240.

(13) Dujardin, E.; Peet, C.; Stubbs, G.; Culver, J. N.; Mann, S. *Nano Lett.* **2003**, *3* (3), 413−417.

(14) Knez, M.; Bittner, A. M.; Boes, F.; Wege, C.; Jeske, H.; Maiss, E.; Kern, K. *Nano Lett.* **2003**, *3* (8), 1079−1082.

(15) Knez, M.; Sumser, M.; Bittner, A. M.; Wege, C.; Jeske, H.; Kooi, S.; Burghard, M.; Kern, K. *J. Electroanal. Chem.* **2002**, *522* (1), 70−74.

(16) Liu, W. L.; Alim, K.; Balandin, A. A.; Mathews, D. M.; Dodds, J. A. *Appl. Phys. Lett.* **2005**, *86* (25), 1−3.

(17) Shenton, W.; Douglas, T.; Young, M.; Stubbs, G.; Mann, S. *Adv. Mater.* **1999**, *11* (3), 253−256.

(18) Balci, S.; Bittner, A. M.; Hahn, K.; Scheu, C.; Knez, M.; Kadri, A.; Wege, C.; Jeske, H.; Kern, K. *Electrochim. Acta* **2006**, *51* (28), 6251−6257.

10.1021/la7016424 CCC: $40.75
Published on Web 12/23/2007

plates[19,20] or genetic modifications that incorporate high-affinity amino acids or substrate-specific peptides[21,22] into the template can enhance biotemplate coatings to produce more uniform metal depositions. For example, modified bacteria M13 viruses have been used to produce hybrid gold−cobalt oxide wires that can enhance battery capacity.[10] Such modifications represent logical starting points for the design of strategies that incorporate biological templates into functional devices.

We have investigated the use of *Tobacco mosaic virus* (TMV) as a template for the deposition of metals. TMV encodes a rod-shaped particle 300 nm in length and 18 nm in diameter with a 4 nm diameter hollow inner channel. Each TMV particle is composed of ∼2130 identical protein subunits of molecular weight 17.5 kDa that self-assemble in a helix around a single strand of genomic virus RNA.[23] TMV particles are also stable in a wide range of temperatures (up to 60 °C) and pH values (∼pH 2−10),[24] making the virus a durable biological template. To enhance mineralization, novel genetic modifications that introduce a cysteine residue onto the amino terminus of each coat protein subunit have been created and found to enhance significantly metal depositions.[22,25]

In this study, TMV genetically engineered to express a novel coat protein cysteine residue, TMV1cys, was used to vertically pattern TMV particles onto gold surfaces via gold−thiol interactions. Studies indicated that TMV1cys readily bound gold surfaces and remained attached during mineralization while the unmodified wild-type virus did not (data not shown). An electroless deposition strategy was used to determine whether surface-assembled TMV1cys could be mineralized in a uniform manner (Figure 1). Previous studies have shown that electroless plating methods can mineralize TMV in solution[26] and that genetically modified viruses encoding novel cysteine residues can significantly enhance the uniformity of metal coatings obtained via this process.[22,25] Patterned TMV1cys virion particles functioned as robust templates for the reductive deposition of nickel and cobalt at room temperature via electroless deposition, producing dense carpets of oriented metal-coated viral templates. Mineralized surface-assembled viruses significantly increased available surface area and enhanced electrode life and voltage output in a battery electrode system. The controlled self-assembly of these virus templates in an oriented manner combined with their enhanced functionalization to produce uniform high surface area electrodes represents a significant advance toward the manufacturing of biologically based devices.

Experimental Section

TMV1cys and Virus Purification. A coat protein mutant, TMV1cys, encoding an additional cysteine residue at the amino terminus of the virus coat protein was used for all experiments.[27] TMV1cys was created by the insertion of a TGT codon in the third amino acid position within the coat protein open reading frame of the full-length TMV infectious clone. *Nicotiana tabacum*, cv Xanthi, a systemic TMV host, was inoculated with infectious RNA transcripts generated from the TMV1cys cDNA clone. Virus was harvested 20 days postinoculation and purified, as previously described.[28] The 1cys insertion in the coat protein open reading frame was verified by cDNA sequencing of reverse-transcribed viral RNA.

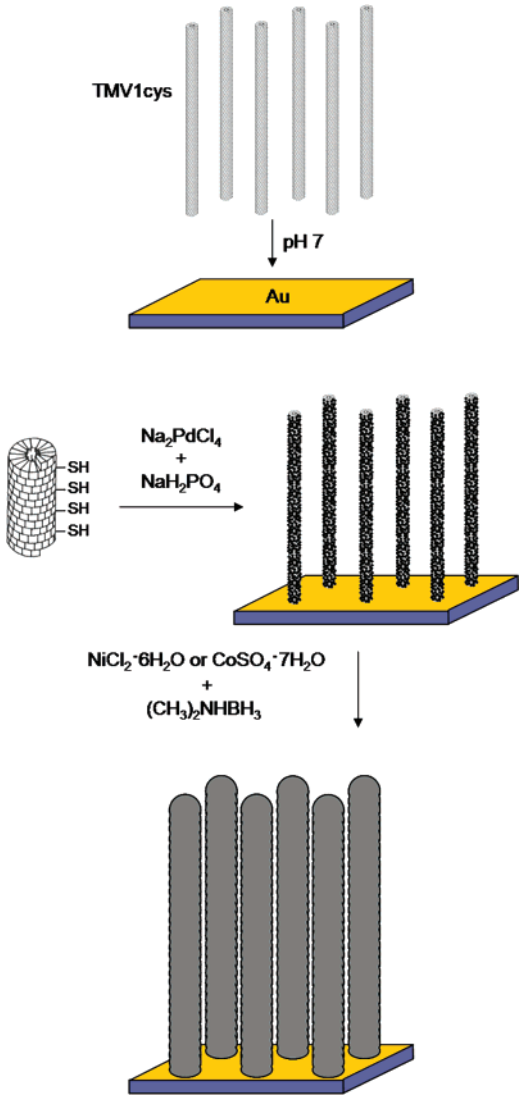

Figure 1. Diagram for the assembly of nickel- and cobalt-coated TMV1cys templates attached to a gold surface.

Surface Assembly and Mineralization. Concentrations of 0.01, 0.1, and 1 mg/mL TMV1cys in 0.1 M pH 7 sodium phosphate buffer in the presence of the gold-coated silicon substrate were allowed to incubate overnight at room temperature. A two-step plating process[14,15,26] was employed to obtain continuous metal deposition on gold surface-assembled TMV1cys. First, TMV1cys templates were activated with a palladium catalyst via the reduction of Pd^{2+} to Pd^0 using a hypophosphite reducing agent. Concentrations of 0.6 mM Na_2PdCl_4 in 0.1 M $NaH_2PO_2{\cdot}H_2O$ in the presence of the template were allowed to incubate overnight. Nickel and cobalt electroless plating solutions, at pH 7 and 9, respectively, were prepared from 0.1 M $NiCl_2{\cdot}6H_2O$ or $CoSO_4{\cdot}7H_2O$, 0.15 M $Na_2B_4O_7$, 0.25 M glycine, and distilled H_2O with a 0.5 M $(CH_3)_2NHBH_3$ reducing agent. Palladium-catalyzed TMV1cys surfaces were submerged in the electroless plating solution for 3−4 min and were then rinsed with distilled water, dried, and stored in air at room temperature. For cross-sectional viewing, a gold-coated mica surface was used, prepared from vacuum-evaporated gold on freshly cleaved mica.

(19) Royston, E.; Lee, S. Y.; Culver, J. N.; Harris, M. T. *J. Colloid Interface Sci.* **2006**, *298* (2), 706−712.
(20) Schlick, T. L.; Ding, Z. B.; Kovacs, E. W.; Francis, M. B. *J. Am. Chem. Soc.* **2005**, *127* (11), 3718−3723.
(21) Lee, S. W.; Mao, C. B.; Flynn, C. E.; Belcher, A. M. *Science* **2002**, *296* (5569), 892−895.
(22) Lee, S. Y.; Royston, E.; Culver, J. N.; Harris, M. T. *Nanotechnology* **2005**, *16* (7), S435−S441.
(23) Namba, K.; Pattanayek, R.; Stubbs, G. *J. Mol. Biol.* **1989**, *208* (2), 307−325.
(24) Stubbs, G. *Semin. Virol.* **1990**, *1*, 405−412.
(25) Lee, S. Y.; Choi, J.; Royston, E.; Janes, D. B.; Culver, J. N.; Harris, M. T. *J. Nanosci. Nanotechnol.* **2006**, *6* (4), 974−81.
(26) Knez, M.; Sumser, M.; Bittner, A. M.; Wege, C.; Jeske, H.; Martin, T. P.; Kern, K. *Adv. Funct. Mater.* **2004**, *14* (2), 116−124.
(27) Yi, H.; Nisar, S.; Lee, S. Y.; Powers, M. A.; Bentley, W. E.; Payne, G. F.; Ghodssi, R.; Rubloff, G. W.; Harris, M. T.; Culver, J. N. *Nano Lett.* **2005**, *5* (10), 1931−1936.
(28) Gooding, G. V.; Hebert, T. T. *Phytopathology* **1967**, *57* (11), 1285ff.

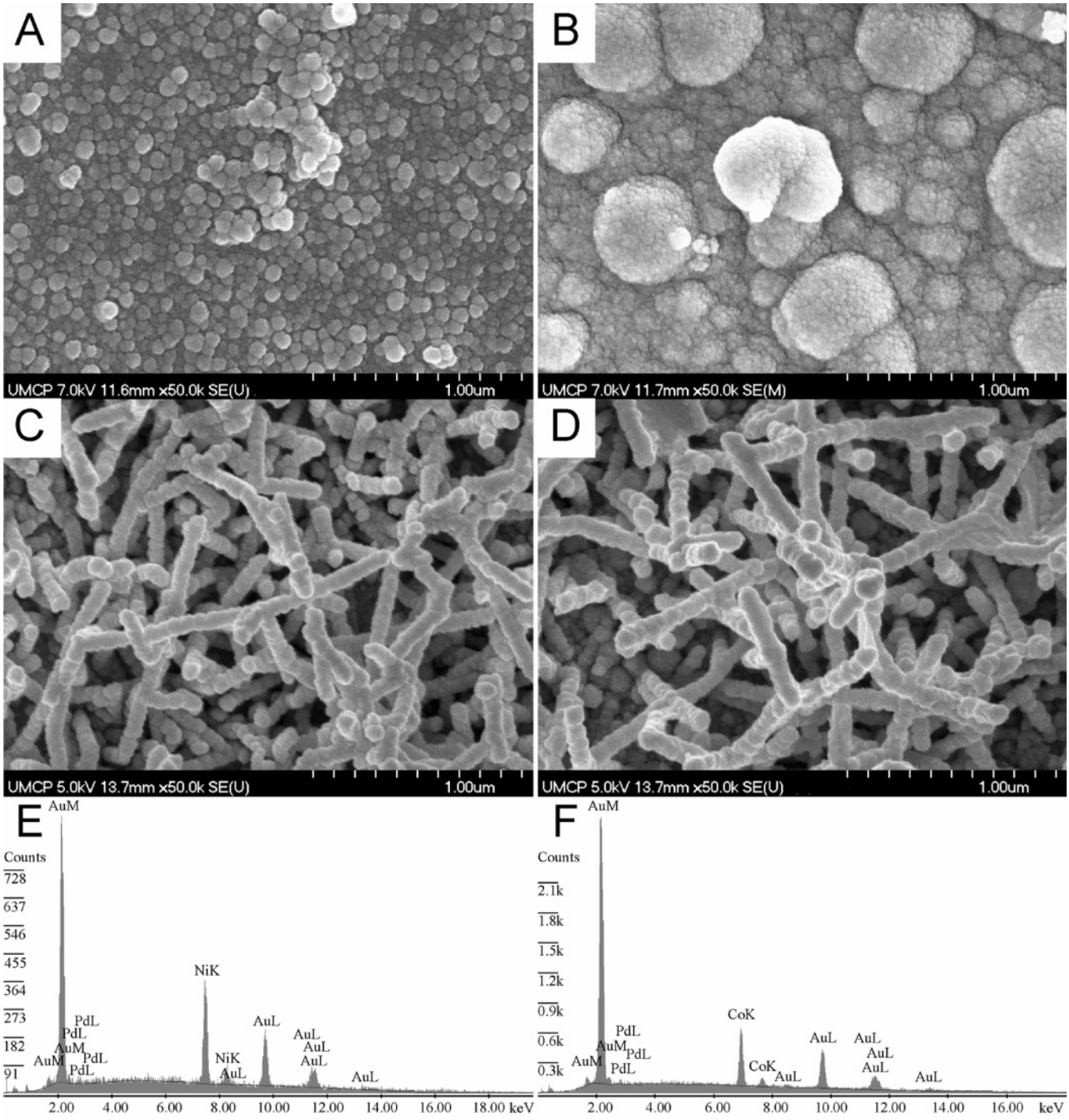

Figure 2. FESEM images showing (a) a nickel-coated gold surface without TMV1cys, (b) a cobalt-coated gold surface without TMV1cys, (c) a nickel-coated gold surface with 1 mg/mL TMV1cys, (d) a cobalt-coated gold surface with 1 mg/mL TMV1cys, and the corresponding EDX spectrum verifying the presence of (e) nickel and (f) cobalt, respectively, for the coated TMV1cys samples.

Nickel-coated Au-mica samples were embedded in Spurr's resin sectioned to 70 nm thickness with a diamond knife. Sections were mounted on a carbon-coated formvar copper grid.

Coating Analysis. Transmission electron microscopy (TEM) images of cross-sectioned nickel-coated TMV1cys attached to a gold-coated mica surface were obtained using a Zeiss EM 10CA transmission electron microscope operated at 80 kV. Field emission electron microscopy (FESEM) images of nickel and cobalt-coated TMV1cys attached to a gold-coated silicon surface were obtained using a Hitachi S-4700 FESEM. Operational parameters ranged 5−20 kV accelerating potential. Energy-dispersive X-ray spectroscopy (EDS) analysis for cobalt or nickel elemental presence was verified using an AMRAY 1820D SEM with an EDAX Genesis EDS system. X-ray photoelectron spectroscopy (XPS) analysis was carried out using a Kratos AXIS Ultra DLD Imaging XPS. High-resolution scans were done for the Ni 2p3/2, O 1s, N 1s, C 1s, and B 1s peaks. All data were acquired using monochromated Al Kα X-rays and processed with CasaXPS software (http://www.casaxps.com). For peak analysis, the nonlinear Shirley background subtraction was employed with curve fittings calculated using a Gaussian−Lorentzian product function. The carbon 1s peak was set to 248.8 eV[29,30] to account for any charging effects.

Battery Assembly and Testing. Electrodes were held in 20 mL of KOH electrolyte with 1 cm spacing between the surfaces. Anodes

(29) Grosvenor, A. P.; Biesinger, M. C.; Smart, R. S.; McIntyre, N. S. *Surf. Sci.* **2006**, *600* (9), 1771−1779.
(30) Siconolfi, D. J.; Frankenthal, R. P. *J. Electrochem. Soc.* **1989**, *136* (9), 2475−2480.

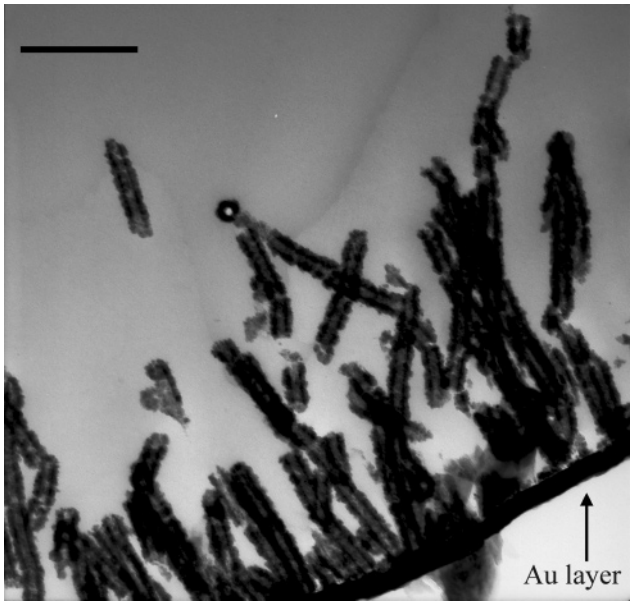

Figure 3. TEM image showing a 70 nm thick cross section of nickel-coated TMV1cys attached perpendicular to a gold-coated mica surface. Coating thicknesses of nickel encasing each particle were measured at ~20 nm. Scale bar is equal to 300 nm.

consisted of 6 cm^2 zinc strips. Gold-coated silicon cut squares 0.5 cm × 0.5 cm, ordered from SPI supplies (West Chester, PA), were used in NiO electrode fabrication. Virus-templated electrode performance was characterized by the repeated charging and discharging of the electrodes using a Solartron 1287A Potentiostat (Hampshire, UK). Electrodes were galvanostatically cycled at a constant rate of 2 mA/cm^2 and between 2.2 and 0.25 V with the discharge capacity calculated in the voltage range 2.2−0.75 V.

Results and Discussion

FESEM analysis clearly showed that surface-assembled TMV1cys templates were continuously coated with nickel and cobalt metals (Figure 2). TMV1cys coating densities measured from FESEM micrographs indicated thicknesses of between 20 and 40 nm of deposited metal encasing each virus particle (Figure 2). Coated surfaces remained stable even after vigorous rinsing to remove excess plating solution. EDS analysis confirmed the presence of nickel or cobalt for surface-assembled TMV1cys templates (Figure 2d and e). Interestingly, surface-assembled TMV1cys templates coated with metal primarily oriented vertically to the gold surface producing carpetlike arrays of coated virus rods. Nickel-coated TMV1cys assembled onto gold-coated mica was thinly sectioned for TEM analysis to confirm this orientation. Results showed the vertical attachment of the virus particles to the gold surface and confirmed nickel coating thicknesses of ~20 nm encasing each particle (Figure 3). In addition, encased virus templates were shown to produce tubes with nickel metal uniformly covering the outer surfaces. One contributing factor in the ability of the virus templates to orient vertically on gold surfaces is the surface topography of TMV, which consists of alternating grooves and ridges that allow the virus to self-align.[23] The position of the 1cys mutation at the third codon position also likely contributes to the vertical positioning of the viral rods on the gold surface. Although surface-exposed, the 1cys mutation is recessed within a groove and partially covered by the C-terminal arm of the coat protein (Figure 4a). This position likely inhibits direct contact between the cysteine-derived thiol and the gold surface, functioning to block virus binding along the outer circumference of the virus particle. However, because the two ends of a TMV particle display different

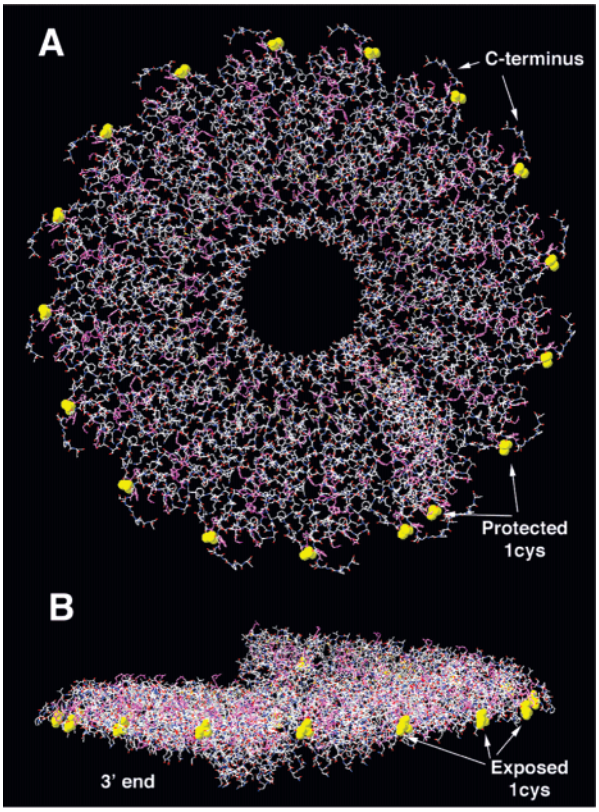

Figure 4. Computer generated model diagramming the position of the 1cys mutations relative to the (a) outer rod surface and (b) the 3′ end.

coat protein surfaces, the position of the 1cys mutation would be sufficiently exposed to make direct contact with the gold surface at the end of the particle that contains the 3′ genome sequence, termed the virus 3′ end (Figure 4b). Additionally, the length of surface-assembled virus rods was on average 700 ± 300 nm or about twice that of an individual TMV1cys particle. The end-to-end alignment of TMV1cys particles can occur readily in solution and would account for the greater than virion lengths observed upon surface assembly and metal coating.[17]

Modulation of the surface assembly of TMV1cys was analyzed under a range of virus concentrations. Figure 5 shows nickel-coated gold surfaces self-assembled using different concentrations of TMV1cys. Increases in the density of surface-assembled TMV1cys particles were observed between a range of 0.01 and 0.1 mg/mL. On the basis of FESEM analysis, concentrations of 0.01 mg/mL resulted in TMV1cys particle counts of 31 ± 4 per μm^2, while both 0.1 mg/mL and 1 mg/mL produced particle counts of 70 ± 10 per μm^2. Using an average deposition thickness of 30 nm and particle length of 700 nm, the calculated increases in surface area are factors of 6 ± 2 for assemblies done at a virus concentration of 0.01 mg/mL and 13 ± 3 for those done at concentrations of 0.1 and 1 mg/mL. These findings demonstrate an ability to tune the surface assembly of TMV1cys and thus potentially control available surface area.

An elemental analysis, using XPS, of nickel-coated TMV templates was performed to determine the suitability of this material to function as a battery electrode. Figure 6 shows high-resolution Ni $2p_{3/2}$ and O 1s spectra from surface-assembled nickel-coated templates. For NiO, a characteristic binding energy peak (BE) is reported at 854.6 eV with a satellite peak at ~861 eV.[31,32] These BEs correspond to peaks of 854.8 and 860.9 eV

(31) Carley, A. F.; Jackson, S. D.; O'Shea, J. N.; Roberts, M. W. *Surf. Sci.* **1999**, *440* (3), L868−L874.

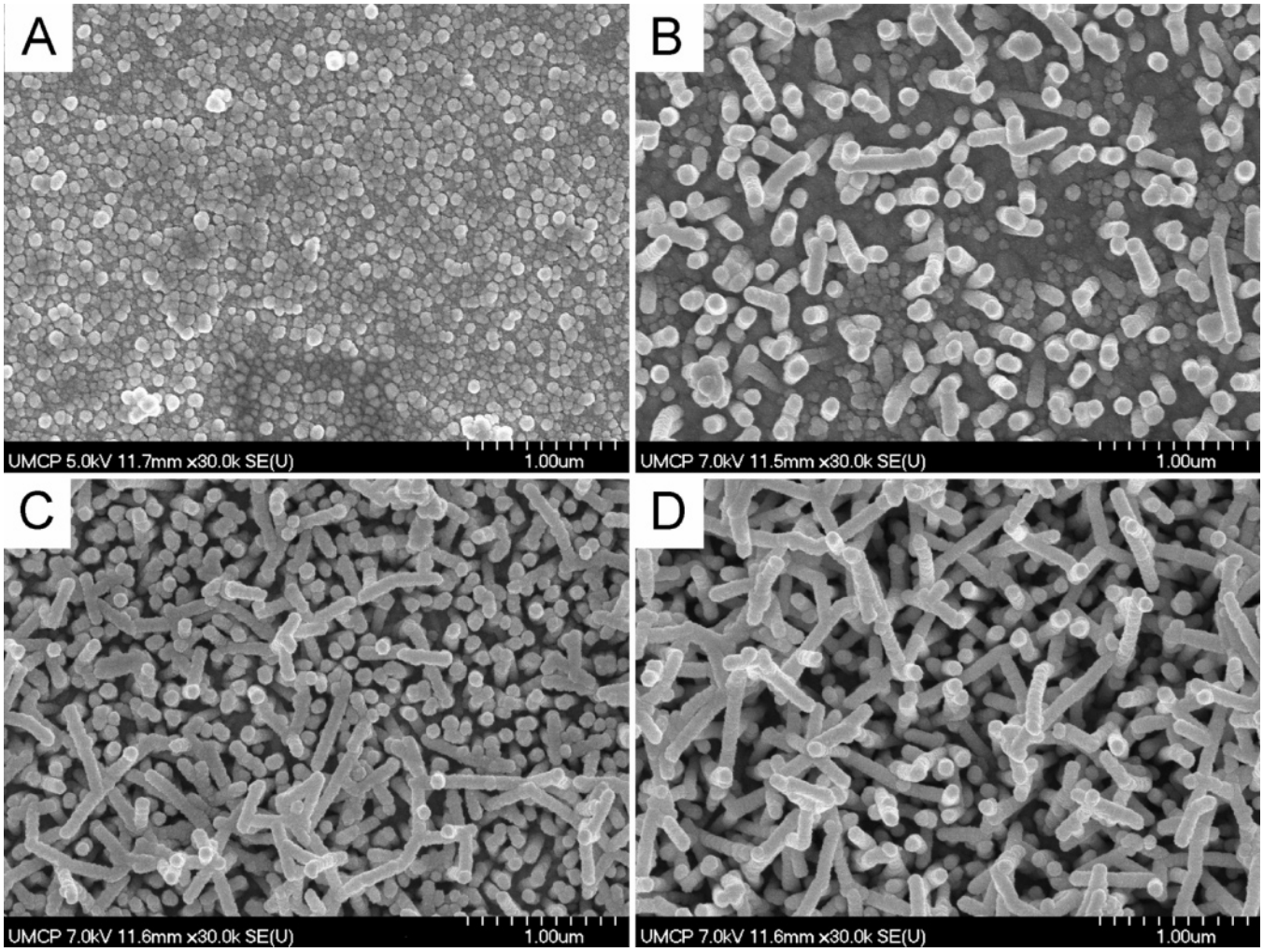

Figure 5. FESEM images showing effects of concentration on the assembly of TMV1cys templates for nickel deposition. Concentrations of (a) 0 mg/mL TMV1cys, (b) 0.01 mg/mL TMV1cys, (c) 0.1 mg/mL, and (d) 1 mg/mL are shown.

measured from the virus-assembled surface, indicating that NiO represented the greatest constituent to the total nickel signal, comprising 18.7% from the main peak and 40.3% from the satellite peak. Additional peaks measured at 855.6, 865.5, and 852.2 eV corresponded to reported BE peaks[29,30] of 855.6 and 865.5 eV for $Ni(OH)_2$ and of 852.2 eV for crystalline Ni. Thus, $Ni(OH)_2$ and Ni constitute 37.6% and 0.9% of the nickel signal obtained from assembled virus surfaces, respectively. Two peaks were assigned from the O 1s spectrum at 530.8 and 531.2 eV, representing contributions of 61.0% and 39.0% of the total oxygen signal. These values were consistent with those reported[30] for the oxygen in NiO and $Ni(OH)_2$, respectively. This elemental analysis indicates that nickel-coated virus surfaces contain levels of NiO sufficient for electrode function.

A NiO−Zn battery system was used to examine electrode activity of surface-assembled virus-coated electrodes. Virus-assembled and control electrodes were created using a 0.25 cm^2 gold-plated silicon wafer base. As the nickel plating process results in the deposition of nickel metal, electrodes were allowed to oxidize for 72 h in air at room temperature prior to testing. Electrode capacity was shown to increase appreciably in the initial 15 cycles with smaller increases continuing to the end of the experiment at 30 cycles (Figure 7a).

Previous work suggests the oxidation of electroless deposited nickel occurs to a depth of at least 6 nm, with an upper surface layer composed of $Ni(OH)_2$.[30] XPS results indicate a similar oxidation state for nickel-coated TMV. From these findings, we expect two electrode chemistries will occur within this battery system as a result of oxidative processes:[33] $2NiOOH + Zn + 2H_2O \rightarrow 2Ni(OH)_2 + Zn(OH)_2$ at 1.73 V and $NiO + Zn \rightarrow Ni + ZnO$ at 1.5 V. The small initial steady discharge observed (Figure 7b) in the region of 1.7 V most likely belongs to the NiOOH reduction reaction, whereas the predominant discharge at the 1.5 V region most likely represents the NiO reduction reaction.

TMV1cys-assembled electrodes consistently outperformed non-TMV1cys-templated electrodes, stabilizing after 15 cycles with a final 2-fold increase in capacity as shown in Figure 7b. Although initial capacity increase showed an order of magnitude improvement for the TMV1cys-templated electrodes over non-TMV1cys-templated electrodes, the swift decrease in capacity to a factor of 2 after 15 cycles may be due to the formation of a passivation layer on the zinc electrode decreasing the active anode surface area.[33] Ab initio calculations based on measurements from electron micrographs indicate $\sim 10^{-4}$ g/cm^2 electrode material is deposited onto the surface of assembled TMV1cys templates. This value was confirmed by microbalance measurements, indicating the presence of 10^{-4} g/cm^2 of deposited nickel on the surface of virus-assembled electrodes. Weight contributions

(32) Hufner, S. *Photoelectron Spectroscopy*; Springer-Verlag: Berlin, 1995.

(33) Linden, D. *Handbook of Batteries*, 2nd ed.; McGraw-Hill Inc.: New York, 1995.

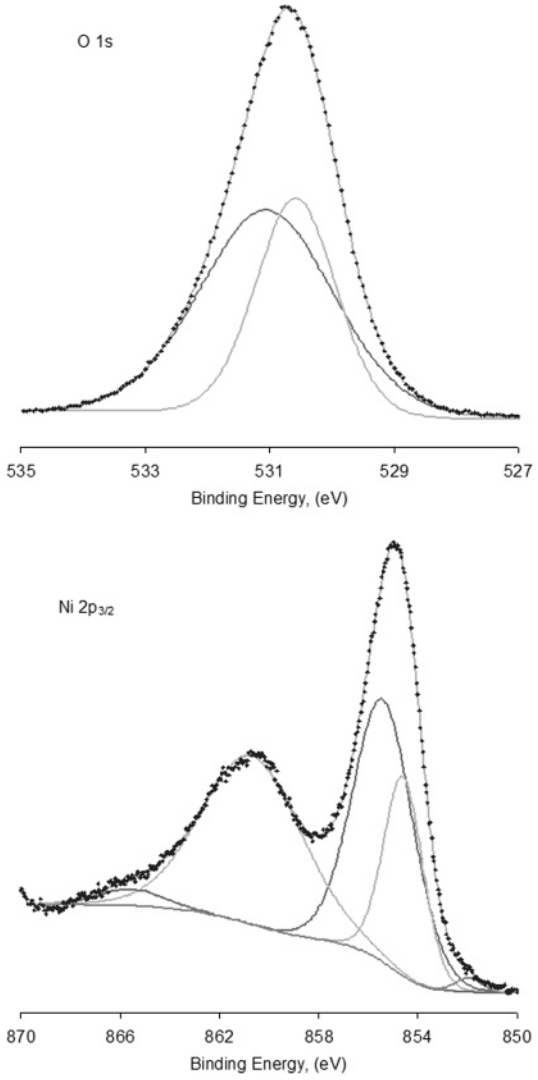

Figure 6. XPS spectrum of the Ni 2p3/2 peaks and O 1s peaks for nickel-coated TMV1cys attached to a gold-coated silicon wafer.

from the virus particles themselves were below the sensitivity limits of the balance and negligible in this calculation. Using these measurements, we calculate a specific discharge capacity on the order of 10^5 mAh/g for the virus-templated electrode surface.

Conclusion

Biologically derived components are unique in that they can encode novel specificities as well as the ability to self-assemble into defined structures. Thus, they have tremendous potential for use in the development and application of a variety of nanoscale devices. One of the challenges in the use of biological components is the ability to integrate these components into devices in a functionally useful way. In this study, we have accomplished the integration of TMV1cys-based nanotemplates onto a solid surface to produce functional high surface area nanomaterials. This self-assembly process works at room temperature and under mild buffer conditions and produces nanostructured materials that are uniformly oriented and coated. The density of surface-assembled virus and thus available surface area was easily tuned by varying the virus concentration of the assembly reaction. A simple electroless deposition method allowed the efficient and uniform metal coating of assembled virus. Once coated, surface attached viruses were highly stable under a variety of conditions including repeated washings with acetone and vacuum drying. This stability

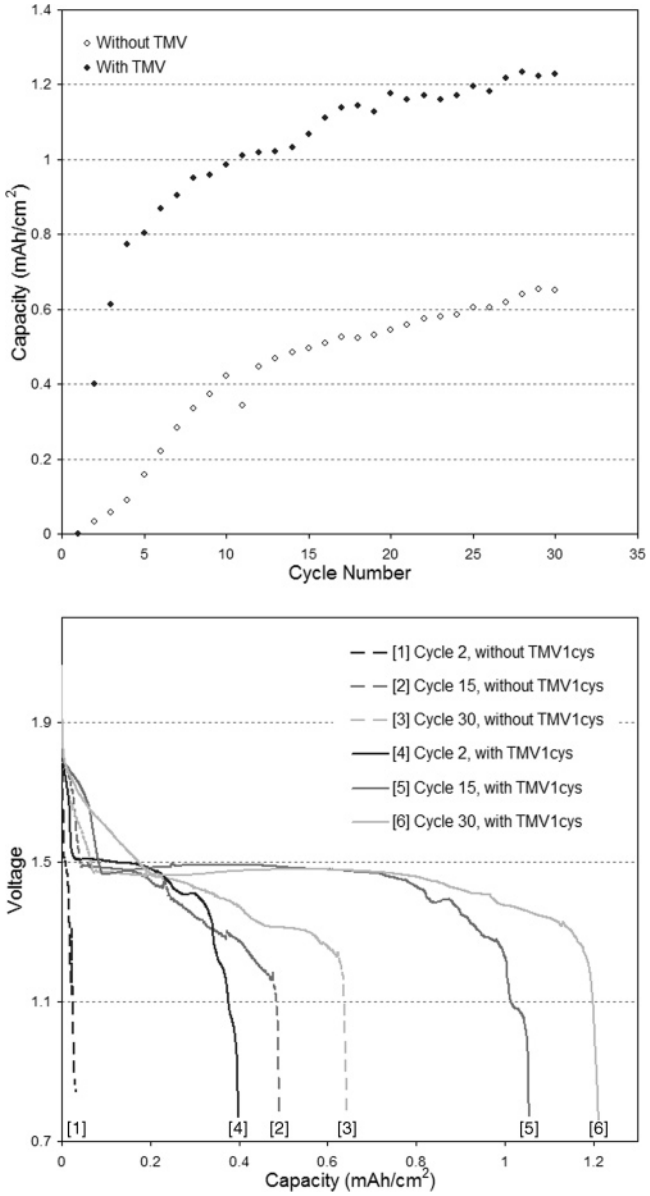

Figure 7. (a) Diagram showing the discharge capacity vs cycle number at 0.2 mA/cm constant current draw for the TMV1cys-templated electrode and the non-TMV1cys-templated electrode. (b) Discharge curves for cycles 2, 15, and 30 at 0.2 mA/cm constant current draw for the TMV1cys-templated electrode and the non-TMV1cys-templated electrode.

was apparent in electrode performance, with FESEM analysis showing no noticeable loss in the structure of the coated viruses after 30 charge−discharge cycles (see Supporting Information). Furthermore, on the basis of observed particle densities this process is efficient with as little as 450 mg of virus required to coat a square meter of electrode surface. Although we have used a simple gold-thiol interaction to assemble these virus templates, previous investigations have demonstrated that TMV can be assembled into more complex patterns using nucleic acid address specific probes derived from the partial disassembly of the virus.[27,34] The combined ability to pattern these templates via several methods could potentially be used to assemble differentially functionalized viruses into complex nanoscale structures.

Acknowledgment. We wish to thank Tim Maugel and Jan Endlich in the Laboratory of Biological Ultrastructure at the

(34) Yi, H.; Rubloff, G. W.; Culver, J. N. *Langmuir* **2007**, *23* (5), 2663−2667.

University of Maryland, College Park, for assistance with EM imaging and sample fixation. We also wish to thank Dr. Dmitry Zemlyanov in the Birk Nanotechnology Center at Purdue University's Discovery Park for assistance in obtaining XPS data and Dr. Yi Liu at the University of Maryland Biotechnology Institute for assistance in analyzing the XPS data. This work was supported in part by DOE awards DEFG02-02ER45975 and 76.

Supporting Information Available: FESEM image showing a nickel-coated TMV electrode after 30 charge/discharge cycles has been included demonstrating the robustness of the electrode surface. This material is available free of charge via the Internet at http://pubs.acs.org.

LA7016424